

1 Revision 1

2

3

4

5

6 A new interpretation of decomposition products of serpentine under shock  
7 compression

8

9 Youjun Zhang<sup>1</sup>, Toshimori Sekine<sup>1, \*</sup> and Hongliang He<sup>2</sup>

10

11 <sup>1</sup>Department of Earth and Planetary Systems Science, Hiroshima University,  
12 Kagamiyama 1-3-1, Higashi-Hiroshima 739-8526, Japan

13 <sup>2</sup>National Key Laboratory of Shock Wave and Detonation Physics, Institute of Fluid  
14 Physics, China Academy of Engineering Physics, PO Box 919-111, Mianyang 621900,  
15 China

16

17

18

19 \*E-mail: [toshimori-sekine@hiroshima-u.ac.jp](mailto:toshimori-sekine@hiroshima-u.ac.jp)

20

21

22

23

## ABSTRACT

24 Dense hydrous magnesium silicates (DHMSs) may play an important role in  
25 water transport during planetary accretion and as water reservoirs in the Earth's deep  
26 mantle. We show that the dynamic decomposition products of antigorite,  
27  $\text{Mg}_3\text{Si}_2\text{O}_5(\text{OH})_4$ , can be interpreted to contain the newly discovered, dense hydrous  
28 silicate, phase H ( $\text{MgSiO}_4\text{H}_2$ ). The Hugoniot for phase H was calculated based on the  
29 Hugoniots for its constituent oxides and the equation of state data derived from first  
30 principles calculations. The measured antigorite Hugoniot, previously suggested to  
31 decompose into high-pressure phases without generating fluid  $\text{H}_2\text{O}$ , was compared  
32 with those derived from calculations involving phase H. Sound velocity data were  
33 also compared to confirm that the dynamic breakdown product of antigorite at  
34 pressures above ~40 GPa is most likely phase H plus MgO without formation of fluid  
35  $\text{H}_2\text{O}$ .

36

37 **Keywords:** Dense hydrous magnesium silicates, Phase H, High pressure, Hugoniot,  
38 Decomposition, Serpentine

39

40

41

## INTRODUCTION

42       Due to their stabilities at high pressures, the dense hydrous magnesium silicates  
43 may provide important insights into deep-focus earthquakes, water sources for the  
44 Earth's interior, and formation of the primitive atmosphere and oceans (e.g., Tyburczy  
45 et al. 1990; Meade and Jeanloz 1991; Ulmer and Trommsdorff 1995; Peacock 2001;  
46 Drake 2005; Kawakatsu and Watada 2007; Sekine et al. 2012). Phase D ( $\text{MgSi}_2\text{O}_6\text{H}_2$ )  
47 previously was thought to be the only possible dense hydrous magnesium silicate  
48 (DHMS) present in the lower mantle (Irifune and Tsuchiya 2007). It has a wide  
49 stability field up to 40–50 GPa in pressure, at temperatures to ~1800 K, dehydrating  
50 to form an assemblage containing perovskite (Pv) and magnesiowustite (Mw) at  
51 higher temperatures (Shieh et al. 1998). Recently, using first principles methods  
52 Tsuchiya (2013) predicted a new high-pressure hydrous phase with composition  
53  $\text{MgSiO}_4\text{H}_2$  as a product of a high-pressure phase transition of phase D. Subsequently,  
54 Nishi et al. (2014) observed this phase (designated phase H) experimentally at ~50  
55 GPa and 920 °C in both quench experiments and *in situ* X-ray diffraction  
56 measurements using multi-anvil apparatuses. At 0 K, phase H is theoretically  
57 predicted to be stable up to ~52 GPa before it dissociates into Pv plus  $\text{H}_2\text{O}$  (ice VIII)  
58 (Tsuchiya 2013). Phase H forms a solid solution with  $\delta\text{-AlOOH}$  and the stability field  
59 of the resulting aluminous phase H (Al) expands to higher pressures and temperatures,  
60 extending into the lower mantle to depths of ~2000 km (Nishi et al. 2014). Shock  
61 wave experiments play an important role in understanding the dynamic behavior of  
62 hydrous minerals and their stability during impact process and can be used to study

63 their potential ability to be a water carrier.

## 64 METHOD AND RESULTS

65 From theoretical calculations (Tsuchiya 2013), phase H is characterized by the  
66 zero-pressure density, bulk modulus, and its first derivative of  $\rho_0 = 3.412 \text{ g/cm}^3$ ,  $K_0 =$   
67  $185.8 \text{ GPa}$ ,  $K'_0 = 4.20$ , respectively, although hydrogen bond symmetrization can be  
68 expected to occur above  $\sim 30 \text{ GPa}$ . A Hugoniot ( $U_s = C_0 + su_p$ ,  $U_s$  shock velocity,  $u_p$   
69 particle velocity, constants of  $C_0$  and  $s$ ) for phase H can be estimated using the  
70 equations of  $C_0 = \sqrt{K_0/\rho_0} = 7.38 \text{ km/s}$  and  $s = (K'_0 + 1)/4 = 1.30$ , respectively.  
71 Moreover, phase H is compositionally a mixture of the phases brucite  $\text{Mg(OH)}_2$  (Br)  
72 plus stishovite  $\text{SiO}_2$  (St) which are stable at our pressures of interest. Therefore, the  
73 Hugoniot for phase H can also be calculated based on the known Hugoniots of Br and  
74 St using the additive volume law. This approach is applicable to estimate Hugoniots for  
75 an isochemical mixture of minerals with known Hugoniots (Al'tshuler and  
76 Sharipdzhanov 1971; Kalashnikov et al. 1973; Telegin et al. 1980). At pressure  $P$ , the  
77 specific volume of the mineral mixture  $V(P)$  can be computed by means of the  
78 relation:

$$79 \quad V(P) = \sum_{i=1}^n \alpha_i V_i(P) \quad (1)$$

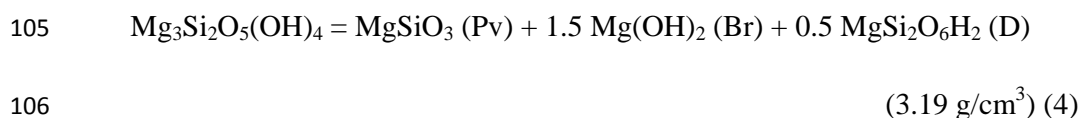
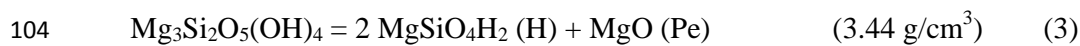
80 Here,  $\alpha_i$  is the weight fraction of mineral  $i$ , and  $\sum_{i=1}^n \alpha_i = 1$ .  $V_i(P)$  is the specific  
81 volume of mineral  $i$ , and can be described as

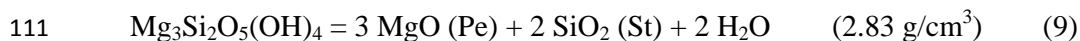
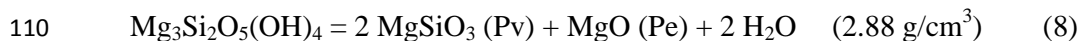
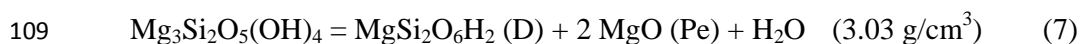
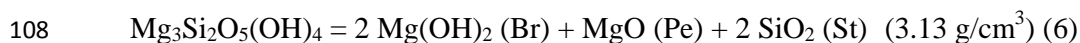
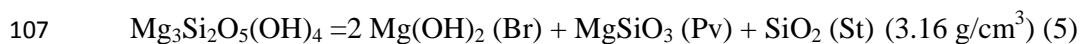
$$82 \quad V_i(P) = \left( 1 - \frac{B_i - \sqrt{B_i^2 - 4A_i}}{2A_i} \right) V_{i,0} \quad (2)$$

83 Therein,  $A_i = s_i^2$ ,  $B_i = 2s_i + C_{i,0}^2/(V_{i,0}P)$ ,  $V_{i,0}$ ,  $C_{i,0}$ , and  $s_i$  are the initial specific  
84 volume, the bulk sound velocity, and the slope of the shock Hugoniot of mineral  $i$  at

85 zero pressure, respectively. Hugoniot parameters calculated for phase H based on both  
86 the results of first principles calculations and the additive volume law, are listed in  
87 Table 1. The calculated Hugoniots are very close to each other for  $P > \sim 40$  GPa. A  
88 predicted Hugoniot for phase D ( $\rho_0 = 3.49 \text{ g/cm}^3$ ) is also calculated from theoretical  
89 equation of state data (Tsuchiya et al. 2005), and listed in Table 1.

90 The Hugoniot for natural antigorite,  $\text{Mg}_3\text{Si}_2\text{O}_5(\text{OH})_4$ , containing small amounts  
91 of  $\text{Al}_2\text{O}_3$ , FeO and  $\text{Fe}_2\text{O}_3$ , has been determined up to a pressure of 140 GPa (Sekine et  
92 al. 2012; Zhang et al. 2014). These results indicate that antigorite shows different  
93 Hugoniots depending on compression duration as shown in Fig. 1. A low-pressure  
94 phase (LPP) exists up to  $\sim 40$  GPa. A metastable extension phase above  $\sim 40$  GPa was  
95 observed in experiments with short compression durations (Fig. 1, open squares for  
96 antigorite in the metastable region ME). In shots with long compression durations, a  
97 decomposition of antigorite occurs above  $\sim 40$  GPa to form high-pressure phase(s)  
98 (HPP). It is consistent with the lizardite data from Tyburczy et al. (1991) (Fig. 1, solid  
99 circles and squares for lizardite and antigorite, respectively). The decomposition is  
100 accompanied by a decrease in density and an increase in sound velocity along the  
101 Hugoniot relative to the metastable extension of the Hugoniot. However, the nature of  
102 the breakdown reactions has not yet been determined fully. Taking into account both  
103 phase D and phase H, possible reactions are as follows;





112 The numbers in parentheses are the calculated zero-pressure densities for the mixtures  
113 on the right-hand side of each reaction. Among these possible breakdown reactions,  
114 we have compared the pressure-density,  $P$ - $\rho$ , relations and sound velocity data to  
115 determine which reaction is the most probable in different pressure intervals.

116 We assumed reactions (5) and (6) with brucite for the high-pressure breakdown  
117 of antigorite (Sekine et al. 2012; Zhang et al. 2014) according to the estimate by  
118 Tyburczy et al. (1991). The zero-pressure densities calculated for the products of  
119 reactions (5) and (6) are 3.16 and 3.13 g/cm<sup>3</sup>, respectively, while the estimated  
120 zero-pressure density is between 3.3 and 4.0 g/cm<sup>3</sup> for HPP of serpentine (lizardite)  
121 (Tyburczy et al. 1991). This suggests we should look for reactions to form more dense  
122 products than reactions (5) and (6). We propose reaction (3) with products of the  
123 zero-pressure density 3.44 g/cm<sup>3</sup> as the most probable decomposition reaction of  
124 antigorite. Hugoniot for decomposition product (3) was calculated based on the  
125 additive volume law using the data listed in Table 1. The results are shown in Figure 1.  
126 As described previously, Hugoniots for phase H were calculated using two  
127 independent methods (Table 1). Predicted Hugoniots for reaction (3) were also  
128 calculated by using the two approaches (shown by symbols + and \* in Fig. 1) and they

129 are located closely. The measured Hugoniot data for antigorite as well as lizardite are  
130 almost on the predicted Hugoniot at pressures of ~40–70 GPa as shown in Fig. 1. So,  
131 in light of the newly discovered phase H, the high-pressure phase of antigorite and  
132 lizardite can be re-interpreted most likely as the product of reaction (3). Further, the  
133 measured Hugoniot data indicate that there appears a gap in the  $P$ - $\rho$  plot at  $P > 70$   
134 GPa, suggesting that phase H may dissociate into Pv and H<sub>2</sub>O (as fluid on the H<sub>2</sub>O  
135 phase diagram (Stewart and Ahrens 2005)), consistent with theoretical calculations  
136 (Tsuchiya 2013). Serpentine may dehydrate by reaction (8) along the Hugoniot, as  
137 indicated by static experiments (Shieh et al. 1998). The calculated Hugoniot for  
138 reaction (8) is plotted in Figure 1 (symbols x) and shows good agreement with the  
139 measured Hugoniot in the pressure range of ~80–125 GPa. The measured Hugoniot is  
140 not consistent with reaction (4) (dash line in Fig. 1), which includes phase D,  
141 probably because the Hugoniot temperature is too low in the stability field of phase D,  
142 or because the reaction is kinetically inhibited. Moreover, phase D is only stable  
143 below ~45 GPa (Irifune and Tsuchiya 2007), thus phase D may not be involved.

144 First principles calculations report similar longitudinal, shear, and bulk sound  
145 velocities for phase D and phase H (Tsuchiya and Tsuchiya 2008; Tsuchiya 2013).  
146 The calculated longitudinal sound velocities of phases D and phase H are 12.2 km/s  
147 and 12.5 km/s at a pressure of 50 GPa, respectively. At ambient pressure, perovskite  
148 and stishovite have high sound velocities, but serpentine, brucite and water have  
149 lower ones. Under ambient conditions, the longitudinal sound velocity of serpentine is  
150 6.76 km/s (Bezacier et al. 2010) and that for the products of reaction (3) is calculated

151 to be 9.6 km/s using the mixing model. The ambient condition values of 9.38 km/s for  
152 phase H (Tsuchiya 2013) and 9.71 km/s for MgO (Zha et al. 2000) were used for  
153 longitudinal sound velocities. This suggests that the reaction product (3) may have a  
154 greater longitudinal velocity than the metastably compressed antigorite. Zhang et al.  
155 (2014) observed an increase in the sound velocity for shocked antigorite above the  
156 decomposition pressure of ~40 GPa. So, the sound velocity increase supports the  
157 occurrence of reaction (3), although they did not measure the sound velocity above 80  
158 GPa.

159 Serpentine (antigorite) is stable up to ~7 GPa at 540 °C (Ulmer and Trommsdorff  
160 1995), and it decomposes or transforms into a series of phases with increasing  
161 pressure. The products vary as a function of pressure and temperature: phase A +  
162 enstatite (En) and phase clinohumite (chu) + En (Stalder and Ulmer 2001), phase D +  
163 superhydrous phase B (sB) ± St, phase D + Pv ± St (Shieh et al. 1998), and phase H +  
164 Pe. The schematic phase boundaries are shown in Figure 2. The stability for phase H  
165 is known to extend substantially in the presence of Al<sub>2</sub>O<sub>3</sub> by forming a solid solution  
166 with δ-AlOOH (Nishi et al. 2014). Hugoniot temperature ( $T_H$ ) of antigorite was  
167 calculated by Zhang et al. (2014) using the relation (Tyburczy et al. 1991):  $T_H =$   
168  $T_0 \exp\left(-\int_{V_0}^V \gamma/V dV\right) + (E_H - E_{tr} - E_S)/C_V$  (therein,  $T_0$  the initial temperature,  $\gamma$   
169 the Grüneisen parameter,  $C_V$  the specific heat,  $E_H$ ,  $E_{tr}$ ,  $E_S$  the Hugoniot energy, phase  
170 transition energy, and isentropic energy, respectively). The calculated  $T_H$  for the  
171 antigorite HPP (Fig. 2) falls within the stability field for aluminous phase H (Al)  
172 above ~40 GPa. Note that the phase boundary for phase H (Al) may have a negative



173 slope. With increasing shock pressure, the temperature will decrease if reaction (3)  
174 proceeds along the boundary. The calculated Hugoniot temperature for antigorite HPP  
175 (Zhang et al. 2014) indicated that it is relatively lower than the calculated temperature  
176 for the metastable extension. Therefore, shock temperature calculation also may  
177 support reaction (3). All the available data prefer the decomposition reaction (3) for  
178 antigorite at pressures of 40–70 GPa, although the decomposition may form  
179 amorphous material of which behaviors are similar to those of the reaction product  
180 (3).

### 181 **GEOPHYSICAL IMPLICATIONS**

182 We conclude that the new high-pressure dense hydrous phase H,  $\text{MgSiO}_4\text{H}_2$ , may  
183 be involved as the decomposition product of serpentine at pressures of ~40–70GPa  
184 and that the reaction does not produce fluid water. It suggests that serpentine can  
185 carry water as phase H to depth of the lower mantle below ~2000 km before  
186 dehydration, and that aluminous phase H (Al) would survive in violent impact events  
187 and at deeper mantle. This implies that serpentine plays a more important role than  
188 previously thought in primitive meteorites and in the Earth's mantle. Although phase  
189 H has never been found in nature, it will have to be recognized as the most stable  
190 hydrous silicate under extreme conditions. If even a trace of water is carried by phase  
191 H near the mantle-core boundary, the water reduces significantly the solidus of  
192 silicates (Nomura et al. 2014) and the temperature estimation at the mantle–core  
193 boundary also will be affected. Under impact conditions, it is unclear whether phase  
194 H formed by decomposition of serpentine is quenchable in the process of pressure

195 release or not. However, serpentine itself has been known to survive in Murchison  
196 carbonaceous chondrite shocked up to a pressure of ~30 GPa (Tomioka et al. 2007).  
197 Therefore, serpentine can be a potential water reservoir to carry water inward the  
198 snowline during the planetary formation. The high pressure and temperature stability  
199 of serpentine and phase H helps us to understand how water is carried to deeper and  
200 hotter areas in the planetary interiors and to the planets near the Sun, although such  
201 water carriers may have been subjected to heat and collision during migration and  
202 accretion.

203

#### 204 **ACKNOWLEDGEMENTS**

205 We thank J. Tsuchiya and M. Nishi for sending their papers and J. Tsuchiya for  
206 providing the calculated sound velocity data for phase H. We are thankful to Ian  
207 Swainson, Paul Asimow, and reviewers for improvement of our draft.

208

#### 209 **REFERENCES CITED**

- 210 Al'tshuler, L.V., and Sharipdzhanov, I.I. (1971) Additive equations of state of silicates  
211 at high pressures. *Izvestiya. Physics of the Solid Earth*, 3, 11-28.
- 212 Bezacier, L., Reynard, B., Bass, J.D., Sanchez-Valle, C., and Van de Moortle, B.  
213 (2010) Elasticity of antigorite, seismic detection of serpentinites, and anisotropy  
214 in subduction zones. *Earth and Planetary Science Letters*, 289, 198-208.
- 215 Drake, M.J. (2005) Origin of water in the terrestrial planets. *Meteoritics & Planetary  
216 Science*, 40, 519-527.

- 217 Duffy, T.S., Ahrens, T.J., and Lange, M.A. (1991) The shock wave equation of state of  
218 brucite  $Mg(OH)_2$ . *Journal of Geophysical Research*, 96(B9), 14319-14330.
- 219 Gong, Z., Fei, Y., Dai, F., Zhang, L., and Jing, F. (2004) Equation of state and phase  
220 stability of mantle perovskite up to 140 GPa shock pressure and its geophysical  
221 implications. *Geophysical Research Letters*, 31, L04614.
- 222 Irifune, T., and Tsuchiya, T. (2007) Mineralogy of the Earth-Phase transitions and  
223 mineralogy of the lower mantle. *Treatise on geophysics*, 2, 33-62.
- 224 Kalashnikov, N., Pavlovskiy, M., Simakov, G., and Trunin, R. (1973) Dynamic  
225 compressibility of calcite-group minerals. *Izvestiya. Physics of the Solid Earth*, 2,  
226 23-29.
- 227 Kawakatsu, H., and Watada, S. (2007) Seismic evidence for deep-water transportation  
228 in the mantle. *Science*, 316, 1468-1471.
- 229 Luo, S.N., Mosenfelder, J.L., Asimow, P.D., and Ahrens, T.J. (2002) Direct shock  
230 wave loading of Stishovite to 235 GPa: Implications for perovskite stability  
231 relative to an oxide assemblage at lower mantle conditions. *Geophysical  
232 Research Letters*, 29, 36-1-36-4.
- 233 Marsh, S.P. (ed) (1980) *LASL Shock Hugoniot Data*. University of California Press,  
234 Berkeley.
- 235 Meade, C., and Jeanloz, R. (1991) Deep-focus earthquakes and recycling of water into  
236 the Earth's mantle. *Science*, 252, 68-72.
- 237 Mitchell, A., and Nellis, W. (1982) Equation of state and electrical conductivity of  
238 water and ammonia shocked to the 100 GPa (1 Mbar) pressure range. *The Journal*

- 239 of Chemical Physics, 76, 6273-6281.
- 240 Nishi, M., Irifune T., Tsuchiya J., Tange Y., Nishihara Y., Fujino K. and Higo Y. (2014)
- 241 Stability of hydrous silicate at high pressures and water transport to the deep
- 242 lower mantle. Nature Geoscience, advance online publication, doi:
- 243 10.1038/ngeo2074.
- 244 Nomura, R., Hirose, K., Uesugi, K., Ohishi, Y., Tsuchiyama, A., Miyake, A., and
- 245 Ueno, Y. (2014) Low core-mantle boundary temperature inferred from the solidus
- 246 of pyrolite. Science, 343, 522-525.
- 247 Peacock, S.M. (2001) Are the lower planes of double seismic zones caused by
- 248 serpentine dehydration in subducting oceanic mantle? Geology, 29, 299-302.
- 249 Sekine, T., Meng, C.M., Zhu, W.J., and He, H.L. (2012) Direct evidence for
- 250 decomposition of antigorite under shock loading. Journal of Geophysical
- 251 Research, 117: B03212.
- 252 Shieh, S.R., Mao, H.-k., Hemley, R.J., and Ming, L.C. (1998) Decomposition of phase
- 253 D in the lower mantle and the fate of dense hydrous silicates in subducting slabs.
- 254 Earth and Planetary Science Letters, 159, 13-23.
- 255 Simakov, G., Pavlovskiy, M., Kalashnikov, N., and Trunin, R. (1974) Shock
- 256 compressibility of twelve minerals. Izvestiya, Physics of the Solid Earth, 8,
- 257 488-492.
- 258 Stalder, R., and Ulmer, P. (2001) Phase relations of a serpentine composition between
- 259 5 and 14 GPa: significance of clinohumite and phase E as water carriers into the
- 260 transition zone. Contributions to Mineralogy and Petrology, 140, 670-679.

- 261 Stewart, S.T., and Ahrens, T.J. (2005) Shock properties of H<sub>2</sub>O ice. Journal of  
262 Geophysical Research, 110, E03005.
- 263 Telegin, G., Antoshev, V., Bugayeva, V., Simakov, G., and Trunin, R. (1980)  
264 Calculated determination of Hugoniot curves of rocks and minerals. Izvestiya.  
265 Physics of the Solid Earth, 16, 319-324.
- 266 Tomoika, N., Tomeoka, K., Nakamura-Messenger, K., and Sekine, T. (2007) Heating  
267 effects of the matrix of experimentally shocked Murchison CN chondrite:  
268 Comparison with micrometeorites. Meteoritics & Planetary Science, 42, 19-30.
- 269 Tsuchiya, J. (2013) First principles prediction of a new high-pressure phase of dense  
270 hydrous magnesium silicates in the lower mantle. Geophysical Research Letters,  
271 40, 4570-4573.
- 272 Tsuchiya, J. and Tsuchiya T. (2008) Elastic properties of phase D (MgSi<sub>2</sub>O<sub>6</sub>H<sub>2</sub>) under  
273 pressure: Ab initio investigation. Physics of the Earth and Planetary Interiors, 170,  
274 215-220.
- 275 Tsuchiya, J., Tsuchiya, T., and Tsuneyuki, S. (2005) First-principles study of hydrogen  
276 bond symmetrization of phase D under high pressure. American Mineralogist, 90,  
277 44-49.
- 278 Tyburczy, J.A., Duffy, T.S., Ahrens, T.J., and Lange, M.A. (1991) Shock-Wave  
279 Equation of State of Serpentine to 150-GPa - Implications for the Occurrence of  
280 Water in the Earths Lower Mantle. Journal of Geophysical Research-Solid Earth,  
281 96, 18011-18027.
- 282 Tyburczy, J.A., Krishnamurthy, R.V., Epstein, S., and Ahrens, T.J. (1990)

- 283 Impact-Induced Devolatilization and Hydrogen Isotopic Fractionation of  
284 Serpentine - Implications for Planetary Accretion. *Earth and Planetary Science*  
285 *Letters*, 98, 245-260.
- 286 Ulmer, P., and Trommsdorff, V. (1995) Serpentine Stability to Mantle Depths and  
287 Subduction-Related Magmatism. *Science*, 268, 858-861.
- 288 Vassiliou, M., and Ahrens, T.J. (1981) Hugoniot equation of state of periclase to 200  
289 GPa. *Geophysical Research Letters*, 8, 729-732.
- 290 Zha, C., Mao, H., and Hemley, R.J. (2000) Elasticity of MgO and a primary pressure  
291 scale to 55 GPa. *Proceedings of the National Academy of Sciences*, 97,  
292 13494-13499.
- 293 Zhang, Y., Sekine, T., Yu, Y., He, H., Meng, C., Liu, F., and Zhang, M. (2014)  
294 Hugoniot and sound velocity of antigorite and evidence for sluggish  
295 decomposition. *Physics and Chemistry of Minerals*, 1-10, doi:  
296 10.1007/s00269-013-0650-0.
- 297
- 298

299 Figure captions

300 **FIGURE 1.** Comparison of pressure-density relations for the measured Hugoniot of  
301 antigorite (squares, not including experimental data based on scaling or “link factors”  
302 calculation, Sekine et al. 2012; Zhang et al. 2014) and lizardite (solid circles,  
303 Tyburczy et al. 1991), and Hugoniots of mixtures of 2 H + Pe (pluses and asterisks), 2  
304 Pv + Pe + 2 H<sub>2</sub>O (crosses), and Pv + 1.5 Br + 0.5 D (dash line). Curves with pluses (+)  
305 and asterisks (\*) represent the calculated Hugoniots for 2 H + Pe by the additive  
306 volume law and by the data derived from the first principles calculations, respectively.  
307 The parameters and references used in the present study are listed in Table 1. LPP and  
308 HPP are the low pressure phase and high pressure phase of antigorite, respectively  
309 (Sekine et al. 2012). Metastable extension (ME) means the Hugoniot of antigorite in  
310 short compression durations and it moves to the HPP in long compression durations  
311 (Sekine et al. 2012). Symbols; H, phase H; D, phase D; Pv, perovskite; Pe, periclase;  
312 Br, brucite; St, stishovite.

313

314 **FIGURE 2.** Schematic illustration of phase boundaries for antigorite in  
315 pressure-temperature plot. Data are after Ulmer and Trommsdorff (1995), Shieh et al.  
316 (1998), Stalder and Ulmer (2001), and Nishi et al. (2014). The calculated Hugoniot  
317 temperature of antigorite is after Zhang et al. (2014). Symbols: A, phase A; Chu,  
318 clinohumite; sB, superhydrous phase B; others, same as in Fig. 1.

319

320

321 **TABLE 1.** Summary of Hugoniot parameters (density  $\rho_0$ , bulk sound velocity  $C_0$ , and  
 322 constant  $s$  at zero pressure) for minerals used in the present study.

323

Minerals	Composition	$\rho_0$ (g/cm <sup>3</sup> )	$C_0$ (km/s)	$s$	Pressures (GPa)	Sources
Brucite (Br)	Mg(OH) <sub>2</sub>	2.382	4.76	1.35	<~100	(Simakov et al. 1974; Duffy et al. 1991) (Marsh 1980;
Periclase (Pe)	MgO	3.584	6.61	1.36	<~200	Vassiliou and Ahrens 1981)
Stishovite (St)	SiO <sub>2</sub>	4.31	9.08	1.23	<~235	(Luo et al. 2002)
Enstatite* (En)	MgSiO <sub>3</sub>	3.06	3.76	1.48	<~140	(Gong et al. 2004)
Water	H <sub>2</sub> O	0.998	2.393	1.333	<~100	(Mitchell and Nellis 1982)
Phase D	MgSi <sub>2</sub> O <sub>6</sub> H <sub>2</sub>	3.49	7.25	1.30	<~40	(Tsuchiya et al. 2005 + This work)†
Phase H	MgSiO <sub>4</sub> H <sub>2</sub>	3.41	7.38	1.30	~40–70	(Tsuchiya 2013 + This work)†
		3.08	5.76	1.31	~40–70	(This work)‡

324 \* Perovskite (Pv) above ~40–50 GPa.

325 † calculated on the results of first principles calculations, respectively.

326 ‡ calculated using the Hugoniot of Br and St by the additive volume law.



Shock pressure (GPa)

